35th Annual International Conference of the IEEE EMBS
Osaka, Japan, 3 - 7 July, 2013

High-resolution MR Imaging of Gastrointestinal Tissue by Intracavitary RF Coil with Remote Tuning and Matching Technique for Integrated MR-endoscope System*

Yuichiro Matsuoka, *Non-member*, *IEEE*, Akihiro Takahashi, *Non-member*, *IEEE*, Etsuko Kumamoto, *member*, *IEEE*, Yoshinori Morita, *Non-member*, *IEEE*, Hiromu Kutsumi, *Non-member*, *IEEE*, Takeshi Azuma, *Non-member*, *IEEE*, Kagayaki Kuroda, *member, IEEE*

***Abstract*— The goal of this study is to establish novel medical technologies by combining magnetic resonance imaging (MRI) with endoscopy to improve diagnostic precision and the safety of endoscopic surgeries. One of the key components of the integrated magnetic resonance (MR) endoscope system is a radio-frequency (RF) coil; this detects the MR signal from tissue and should be placed inside the body. Resonance characteristics such as the resonant frequency and the impedance of the RF coil, which affect the quality of MR images, change depending on the electric properties of the surrounding tissue and the coil deformation. Therefore, the technique of remote tuning and matching of the RF coil was developed, and its feasibility was investigated using a developed intracavitary RF coil, 1.5 tesla MR scanner, and models of phantom and resected porcine stomach. As a result, the frequency tuning and impedance matching was remotely adjusted in both models. In addition, the signal-to-noise ratio (SNR) of MR images was improved up to 134%. The developed remote tuning and matching technique was able to adjust the resonant characteristics of RF coil and can contribute the improvement of MR image quality, which would facilitate safe and precise endoscopy and endoscopic surgeries.**

I. Introduction

Gastrointestinal (GI) cancer death has been ranked highly among causes of death by cancer. Cancer of the esophagus, stomach, and colon has a particularly high prevalence in Japan. Early detection of GI lesions is essential to improve the efficacy of GI cancer therapy and to reduce mortality. Endoscopes represent an invaluable imaging tool for early diagnosis. Moreover, recently developed endoscopic surgeries, such as endoscopic submucosal dissection (ESD) [1], have become a powerful therapy for the early stage of GI cancer if the lesion infiltrates the submucosal layer. The accuracy of preoperative endoscopy of the lesion is needed for precise and safe endoscopic surgeries like ESD; however, preoperative diagnosis using endoscopic ultrasound (EUS) [2] and magnifying endoscopy is not sufficiently accurate. Furthermore, endoscopic surgeries could entail some risks, such as bleeding, perforation, and even death during the procedure. Among endoscopists, expert skills and proficiency in advanced endoscopic surgeries are required. Hence, new medical technologies need to be developed in order to enhance the safety and reliability of endoscopy and endoscopic surgeries.

An endoscope shows the surface information of the target tissue, but does not provide cross-sectional images. The visualization of tissue under the surface is very important in terms of precise diagnosis and preoperative planning. Imaging modalities such as EUS, optical coherence tomography (OCT), magnifying endoscopy, infrared imaging (IRI), and narrow band imaging (NBI) have been developed to overcome this limitation. EUS provides cross-sectional images of deep-lying regions in real-time; however, it has difficulty obtaining high-contrast images of soft tissue. In addition, the image quality of EUS depends on the operator's skill. OCT, magnifying endoscopy, IRI, and NBI provide useful and precise information when it comes to diagnosing the superficial region in the mucosa of GI tissue, but do not depict deep-lying regions.

On the other hand, magnetic resonance imaging (MRI) provides cross-sectional and high soft-tissue contrast images with free slice orientations; moreover, it does not use ionizing radiation. Therefore, the final goal of this study was to develop an MR-endoscope system by integrating the endoscope into MRI to provide high-resolution MR imaging during endoscopy and to navigate both MR imaging and endoscopy [3]. This system required a radio-frequency (RF) coil used to receive MRI signals while inserted into GI tract, tracking sensors to detect the positions of the RF coil and the endoscope tip inside body, and navigation software [4] to show both MRI and endoscope images.

MRI uses RF coils, which are usually placed around the body near the target region. The MR image quality depends on several factors, including the distance from the RF coil to the

*Research supported by Intellectual Ventures.

Y. Matsuoka was with the Department of Research and Development, Foundation for Kobe International Medical Alliance, Kobe, 6500046 JAPAN (corresponding author to provide phone: +81-78-381-5110; fax: +81-78-303-6224; e-mail: matsuoka@kobeima.org), and now is with the Center for Information and Neural Networks (CiNet), National Institute of Information and Communications Technology, Suita, 565-0871 JAPAN (phone: +81-80-9098-3233; fax: +81-6-7174-8616; e-mail: yuichiro_matsu@nict.go.jp)

A. Takahashi is with the Graduate School of System Informatics, Kobe University, Kobe, 6578501 JAPAN (e-mail: 120x017x@stu.kobe-u.ac.jp).

E. Kumamoto is with the Information Science and Technology Center, Kobe University, Kobe, 6578501 JAPAN (e-mail: kumamoto@kobe-u.ac.jp).

Y. Morita, H. Kutsumi, and T. Azuma are with the Division of Gastroenterology, the Department of Internal Medicine, Kobe University Graduate School of Medicine, Kobe, 6500017 JAPAN (e-mail: ymorita@med.kobe-u.ac.jp, hkutsumi@med.kobe-u.ac.jp, and azumat@med.kobe-u.ac.jp).

K. Kuroda is with the School of Information Science and Technology, Tokai University, Hiratsuka, 2591292 JAPAN (e-mail: kagayaki@keyaki.cc.u-tokai.ac.jp).

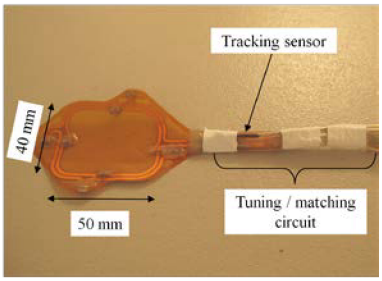

Figure 1. Intracavitary RF coil

target region, the frequency tuning and impedance matching of the RF coil, and the static magnetic field strength of the MR system [5-7]. The wall of the GI tract is very thin and located deep in the body; therefore, MR imaging using conventional RF coils placed outside the body is not sufficient to obtain high-quality, cross-sectional images of the GI wall, as the signal-to-noise ratio (SNR) decreases with the distance from the RF coil. To obtain high-quality MR images of the GI tract, we developed a receive-only flexible intracavitary RF coil for the MR-endoscope system, to be placed inside the GI tract [3]. However, when this coil is inserted into the GI tract, and particularly the stomach, several difficulties emerge in terms of preserving the appropriate frequency tuning and impedance matching, as well as controlling the shape and position of the RF coil inside the stomach. The resonant characteristics of the RF coil usually change depending on its deformation and the electric properties of the surrounding tissue. Thus, new technologies are required to adjust the resonant characteristics of the intracavitary RF coil, and to control its shape and position inside the GI tract. Therefore, remote frequency tuning and impedance matching technique to adjust the resonant characteristics of the intracavitary RF coil placed inside the stomach was developed, and the performance of the system was examined using a phantom and resected porcine stomach.

II. Methods and Materials

A. The RF Coil and Frequency Tuning/Impedance Matching

The intracavitary RF coil that was used, as shown in Fig. 1, was designed as a two-turn flexible surface structure of about 40 × 50 mm^2 and composed of copper; it was 2 mm in width and 0.035 mm in thickness [3]. The coil element was rigidly wrapped with a polyimide substrate of a thickness of 0.025 mm, and every electrical part was coated with silicone to avoid electrical leakage. An RF coil must be tuned to the resonance frequency (Larmor frequency; f_0) of the signal of the target nucleus, most likely hydrogen nucleus or proton, determined by the static magnetic field strength of the MR system (i.e., about 64 MHz at 1.5 Tesla). Moreover, the impedance of the RF coil must be much matched to the characteristic impedance of the coaxial cable (typically 50 Ω) in order to maximize the efficiency in the signal reception and thus the SNR. The frequency tuning and impedance matching of the RF coil are usually achieved with a resonant circuit including non-magnetic capacitors placed right near the RF coil (Fig. 2). A non-magnetic PIN diode is used to achieve decoupling of the RF coil during RF excitation. This

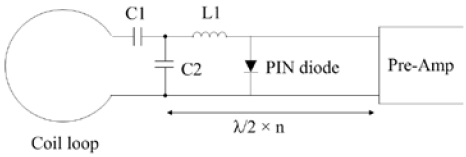

Figure 2. Schematic of the common frequency tuning and impedance matching circuit for the RF coil.

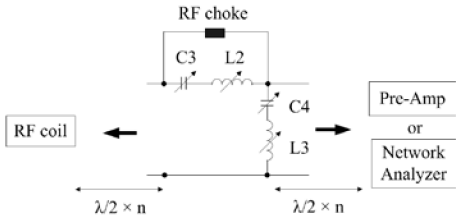

Figure 3. Schematic of the remote frequency tuning and impedance matching circuit.

frequency tuning and impedance matching circuit was placed near the coil loop. Then, the resonant frequency and impedance of the RF coil were roughly tuned and matched to the target values, which should be f_0 and 50 Ω. This was done because the resonant frequency and impedance of the RF coil usually shift when the RF coil is inserted into the body, which causes the change of the loading to the RF coil and the deformation of the RF coil.

B. Remote Frequency Tuning/Impedance Matching

The remote frequency tuning and impedance matching circuit for the receive-only intracavitary RF coil was designed using non-magnetic variable capacitors, inductors, and RF choke (Fig. 3). Based on electromagnetic theory, the electrical properties at the end of a coaxial cable with n times the half wavelength (λ/2 × n) of the signal are identical. In this study, we used 1.5 Tesla MRI (Signa EXCITE TwinSPEED ver.11, GE Heathcare, USA). Therefore, the half wavelength (λ/2) of the coaxial cable (ECX 0.8D-2V, Tachii Electric Wire Co., Ltd., JAPAN) with polyethylene as a dielectric was about 1.5 m. Applying this impedance transformation, the remote frequency tuning and impedance matching circuit could be placed outside the body and away from the magnet of the MRI system. Measurement of the resonant characteristics of the intracavitary RF coil was performed with a Network Analyzer (8714ES, Agilent Technologies, Inc., USA) outside the MR scanner room using the λ/2 × n coaxial cable to connect them. The remote frequency tuning and impedance matching of the intracavitary RF coil were performed by manually changing the values of the variable capacitors and inductors while monitoring the coil resonance curve.

C. MR Imaging and SNR Evaluation

Two subjects, described below, were used to assess the adjustability of the resonant characteristics of the intracavitary RF coil by the remote frequency tuning and impedance matching circuit, and to evaluate the improvement of SNR in relation to MR image quality.

TABLE I. RESONANT CHARACTERISTICS WITH OR WITHOUT REMOTE TUINING AND MATCHING UNDER DIFFERENT LOADINGS

Loading	Remote Tuning and Matching	Resonant characteristics						
		Frequency (MHz)	Impedance (Ω)	Q Factor	Smith Chart		Standing Wave Ratio	Return Loss (dB)
					Resistance (Ω)	*Reactance (Ω)*		
Air (Unload)	Without	64.500	84.5	81.8	84.3	6.3	1.70	11.7
$CuSO_4$ Phantom	Without	64.405	69.2	67.9	67.8	14.0	1.47	14.4
	With	63.865	48.3	67.7	48.3	-1.8	1.05	31.9
Resected Porcine Stomach	Without	63.325	60.6	58.1	58.7	15.0	1.38	16.1
	With	63.865	50.3	51.7	50.3	2.1	1.04	33.4

(1) $CuSO_4$ phantom, composed of NaCl of 0.79 ± 0.05 g, $CuSO_4$-$5H_2O$ of 0.35 ± 0.05 g, and distilled water of 175 ml.

(2) Resected stomach from healthy pig placed on the lard block. The stomach was incised along the lesser curvature, and then the intracavitary RF coil was placed on the mucosa near the pylorus on the side of the greater curvature.

The resonant characteristics of the intracavitary RF coil under loaded conditions were measured by the Network Analyzer at S11 measurement before and after remote frequency tuning and impedance matching were performed. The MR imaging was executed using the following sequences:

(a) Fast spin echo (FSE) with repetition time (TR), 500 ms; echo time (TE), 18.9 ms; echo train length (ET), 4; readout bandwidth (RBW), 15.6 kHz; field of view (FOV), 8 × 8 cm; slice thickness, 5 mm; acquisition matrix, 256 × 128; signal acquisition, 1 in the T1-weighted images for the $CuSO_4$ phantom.

(b) FSE with TR, 3000 ms; TE, 105.6 ms; ET, 18; RBW, 15.6 kHz; FOV, 6 × 6 cm; slice thickness, 3 mm; acquisition matrix, 256 × 256; and signal acquisition, 6 in the T2-weighted images for the resected porcine stomach.

The navigation developed for the integrated MR-endoscope system was applied to recognize the MR scanning range without common scout imaging. A tracking sensor (EndoScout, Robin Medical Inc., USA) based on the native gradient fields of the MR scanner and mounted on the intracavitary RF coil was used to recognize the RF coil position before and after the remote frequency tuning and impedance matching, and to set the MR scanning range by the navigation [4].

The SNRs of MR images were computed by measuring the mean signal intensity (SI) from region of interest (ROI) in the CuSO4 phantom or the resected porcine stomach and standard deviation (SD) from ROI in the background, defined as:

$$SNR = (SI \text{ of } ROI) / (SD \text{ of background }). \quad (1)$$

III. RESULTS

A. Resonant Characteristics

The resonant characteristics of the intracavitary RF coil with and without remote frequency tuning and impedance matching at different loadings are shown in Table I. The resonant characteristics of the RF coil shifted greatly when the resected porcine stomach was loaded. Moreover, the frequency tuning and impedance matching of the intracavitary RF coil were correctly adjusted with the remote frequency tuning and impedance matching circuit. When the resected porcine stomach was loaded, a quality (Q) factor of over 50 was achieved. The shifts of the intracavitary RF coil position before and after the remote frequency tuning and impedance matching were almost zero at the loading of CuSO4 phantom and less than 2.0 mm at the resected porcine stomach loading.

B. MR Images and SNR

Figures 4 and 5 show the MR images of the $CuSO_4$ phantom and resected porcine stomach before and after the remote adjustment of the frequency tuning and impedance matching. The spatial resolutions of the MR image were 0.313 × 0.625 × 5 mm^3 for the $CuSO_4$ phantom and 0.234 × 0.234 × 3 mm^3 for the resected porcine stomach, respectively. In each image, the window width and window level to adjust the contrast and brightness of the image were consistent. Several layers of the stomach wall could be depicted, and were especially clearly visualized in the T2-weighted images of the resected porcine stomach, as shown in Fig. 5.

The SNR distribution in the MR images of the $CuSO_4$ phantom is shown in Fig. 6. The SNRs were obtained at different positions from the intracavitary RF coil by measuring the mean signal intensities of ROIs placed in five different positions. Using remote frequency tuning and impedance matching, the SNR of the MR image could be improved up to about 131%. Regarding the resected porcine stomach, the SNRs in each layer were calculated by measuring the mean signal intensities of ROIs placed in each layer (Fig. 7). The achievement of precise frequency tuning and impedance matching resulted in the SNR improvement of the MR images up to about 134% for the T2-weighted images.

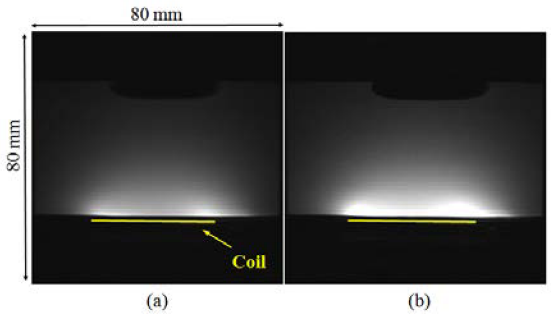

Figure 4. T1-weighted image of $CuSO_4$ phantom. Here, (a) and (b) show images obtained before and after the achievement of the remote frequency tuning and impedance matching, respectively.

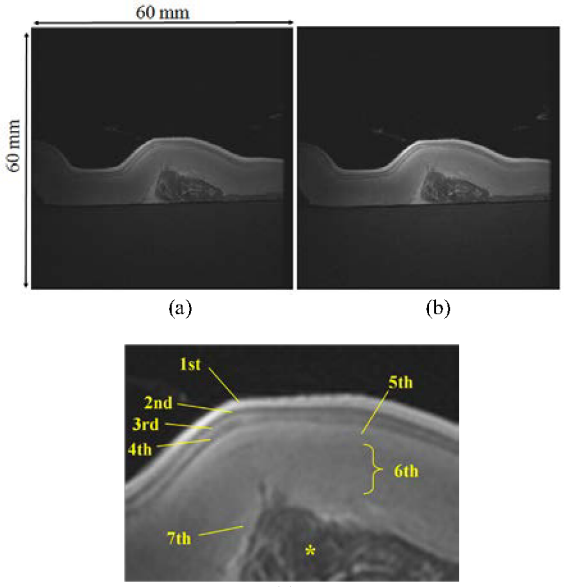

Figure 5. T2-weighted image of resected porcine stomach. Here, (a) and (b) indicate images obtained before and after the achievement of the remote frequency tuning and impedance matching, respectively, while (c) shows the enlarged image of the cross-sectional region of the stomach wall; each layer distinguished in this image is indicated. * corresponds to the greater omentum.

IV. Discussion

The Larmor frequency of the MRI system used in this study was 63.865 MHz. The intracavitary RF coil was roughly tuned and matched to this Larmor frequency and the characteristic impedance of the coaxial cable in the unloaded condition. The deformation of the intracavitary RF coil was not confirmed at the loading of the $CuSO_4$ phantom. Therefore, the dielectric properties of the $CuSO_4$ phantom might induce a change in the resonant characteristics of the intracavitary RF coil from that in the unloaded condition. On the other hand, the shape of the intracavitary RF coil bent slightly at the loading of the resected porcine stomach. This deformation of the coil shape, in addition to the dielectric properties of the resected porcine stomach tissue, might cause a great deal of change in the resonant characteristics of the intracavitary RF coil. Using the remote frequency tuning and impedance matching circuit, the resonant frequency and impedance of the

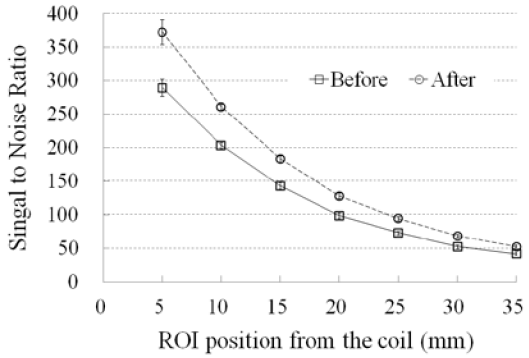

Figure 6. SNRs distribution in $CuSO_4$ phantom image.

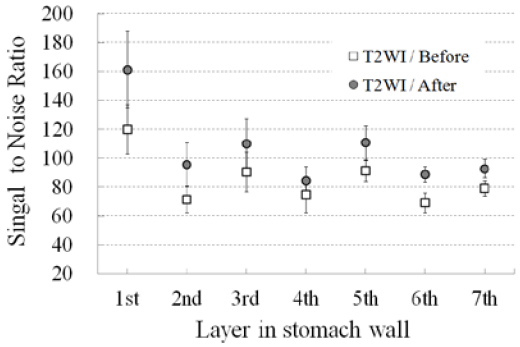

Figure 7. SNRs in T2-weighted images before and after remote frequency tuning and impedance matching were performed.

intracavitary RF coil were correctly adjusted. The developed remote frequency tuning and impedance matching technique for the intracavitary RF coil was demonstrated to compensate for the shift of the resonant frequency, with at least ±0.540 MHz, and of the impedance, with 20.9 Ω. In the ideal frequency tuning and impedance matching, the standard wave ratio (SWR) must be close to 1.0, while the return loss should be as large as possible. The improvement of the SWR and return loss also demonstrated that precise frequency tuning and impedance matching were achieved.

The achievement of precise, remote frequency tuning and impedance matching of the intracavitary RF coil could contribute to the enhancement of the SNR of MR images. The sensitivity of the surface-type RF coil decreases with distance from the coil surface [7]. Generally, the sensitive depth of the surface-type RF coil is about a radius of the coil loop from the center of the coil surface [6, 8], and is almost equal to the position in which the sensitivity is about 35% of maximum sensitivity [5]. The result of the SNR distribution of $CuSO_4$ phantom image (Fig. 6) was consistent with this theory, even when remote frequency tuning and impedance matching were achieved.

The thickness of the resected porcine stomach wall used in this study was about 10 mm, which was within the sensitive depth of the intracavitary RF coil used in this study. Therefore, the intracavitary RF coil could effectively depict the cross-sectional structure of the resected porcine stomach. In addition, the precise adjustment of the resonant characteristics of the intracavitary RF coil by the remote frequency tuning and impedance matching contributed to improving the MR image quality of the resected porcine stomach. The

improvement of SNR in the stomach wall region was at least 113% in the fourth layer and up to 134% in the first layer in T2-weighted images. Thus, the good performance of remote frequency tuning and impedance matching of the intracavitary RF coil was demonstrated in the experiment with the phantom and the resected porcine stomach. The feasibility of adjusting the frequency tuning and impedance matching remotely should be examined with an animal experiment in vivo in future work.

Several techniques related to remote frequency tuning and impedance matching of the RF coil has been developed; however, those techniques have been designed using variable capacitor like a varactor, not using variable inductor [9-12]. In this study, remote frequency tuning and impedance matching were adjusted by manually changing the value of the variable capacitors and inductors. It took several minutes to achieve the frequency tuning and impedance matching. Therefore, an automatic remote adjustment system that can complete the frequency tuning and impedance matching within a few seconds should be developed to make the integrated MR-endoscope system truly useful. Additionally, a control system respecting the shape and position of the intracavitary RF coil inside the body should be developed. These issues will be solved in the next step in our overall research. An integrated MR-endoscope system including these functions will contribute to the safety and accuracy of minimally invasive therapy, in addition to bringing about the reduction of patients' risk.

REFERENCES

[1] T. Gotoda, H. Yamamoto, RM. Soetikno, "Endoscopic submucosal dissection of early gastric cancer," *J Gastroenterol.*, vol. 42, pp. 42-47, 2006.

[2] M. F. Byrne, P. S. Jowell, "Gastrointestinal imaging: endoscopic ultrasound," *Gastroenterology*, vol. 122, pp. 1631-1648, 2002.

[3] H. Yoshinaka, Y. Morita, Y. Matsuoka, D. Obata, S. Fujiwara, R. Chinzei, M. Sugimoto, T. Sanuki, M. Yoshida, H. Inokuchi, E. Kumamoto, K. Kuroda, T. Azuma, H. Kutsumi, "Endoluminal MR imaging of porcine gastric structure in vivo," *J Gastroenterol.*, vol. 45, pp. 600-607, 2010.

[4] Y. Matsuoka, E. Kumamoto, A. Takahashi, Y. Morita, H. Kutsumi, T. Azuma, K. Kuroda, "Navigation of quick MR scanning setup with intraluminal RF coil for integrated MR-Endoscope system," in *Proc. 20th Annual Meeting & Exhibition on ISMRM*, Melbourne, 2012, p. 1590.

[5] A. Haase, F. Odoj, M. V. Kienlin, J. Warnking, F. Fidler, A. Weisser, M. Nittka, E. Dommel, T. Lanz, B. Kalusche, M. Griswold, "NMR probeheads for in vivo applications," *Concepts in Magnetic Resonance,* vol. 12, pp. 361-88, 2000.

[6] A. Haase, W. Hänicke, J. Frahm, "The influence of experimental parameters in surface-coil NMR," *J Magn Reson.*, vol. 56, pp. 401-12, 1984.

[7] M. R. Bendall, "Surface coil technology," in *Magnetic Resonance Imaging*, C.L. Partain, editor. Philadelphia: Saunders, 1988, pp. 1201-68.

[8] B. H. Suits, A. N. Garroway, J. B. Miller, "Surface and gradiometer coils near a conducting body: the lift-off effect," *J Magn Reson.*, vol. 135, pp. 373-379, 1998.

[9] J. L. Ackerman, E. Nevo, J. Zucker, A. J. Poitzsch, K. Vandenberg, A. Zhigalin, B. Fetics, "MR endoscope with software-controlled tuning, device tracking and video," in Proc. *19th Annual Meeting & Exhibition on ISMRM*, Montreal, 2011, p. 1759.

[10] B. L. Beck, S. Wu, W. J. Turner, R. Bashirullah, T. H. Marei, "High Q reactive network for automatic impedance matching," in Proc. *19th Annual Meeting & Exhibition on ISMRM*, Montreal, 2011, p. 1853.

[11] C. Snyder, C. Rogers, L. DelaBarre, M. Robson, J. Vaughan, "Remote tuning and matching an 8-channel transceiver array at 7T," in Proc. *19th Annual Meeting & Exhibition on ISMRM*, Montreal, 2011, p. 3811.

[12] S-M. Sohn, A. Gopinath, J. T. Vaughan, "Electrically auto-tuned RF coil design," in Proc. *19th Annual Meeting & Exhibition on ISMRM*, Montreal, 2011, p. 3826.